Performance Analysis of PEMFC Based Grid-connected Distributed Generation System

Alper Nabi AKPOLAT (alper.nabi@marmara.edu.tr)
Department of Electrical-Electronics Engineering, Faculty of Technology, Marmara University, 34722, Istanbul, Turkey https://orcid.org/0000-0002-6972-2509
Erkan Dursun
Marmara University

Original article

Keywords: Distributed generation (DG), Fuel cell, Wind turbine, Photovoltaic (PV), Performance analysis

Posted Date: October 23rd, 2020

DOI: https://doi.org/10.21203/rs.3.rs-95537/v1

Performance analysis of PEMFC based grid-connected distributed generation system

Alper Nabi Akpolat*, Erkan Dursun

[1]Department of Electrical-Electronics Engineering, Faculty of Technology,
Marmara University, 34722, Istanbul, Turkey
alper.nabi@marmara.edu.tr, erkandursun@marmara.edu.tr

*Corresponding Author

Abstract

Background: Less energy consumption and more efficient use of fossil-fueled technologies are among the sustainable energy targets of modern societies. The essential activities to be achieved under these objectives are to increase the distributed generation structures and increase their applicability. The distributed generation (DG) is a small-scale version of the traditional power grid, which is supported by micro turbines, hydrogen fuel cells, wind turbines, photovoltaic (PV) modules, combine heat and power systems, and energy storage units.

Methods: The aim of this research is to detail performance analyze and unit sizing of proton-exchange membrane fuel cell (PEMFC)-based grid-connected distributed generation system with the help of empirical calculations. To this end, we tried to establish the system and analyze the performance of reliable operation of the system with experimental verifications.

Results and Conclusions: The results demonstrate the situation of annual production about how much rated power can be generated through the real meteorological data to dispatch the power to the constant variable loads. While, 53.56% of the total energy demand is met by the utility grid, 46.44% of the demand is met by the produced energy i.e., from microgrid. The PEMFC based hybrid microgrid at Marmara University, Faculty of Technology was analyzed in detail in this study. According to the results of the performance analysis, the important points that will be highlighted and will help the researchers working in this field are as follows. Our results are encouraging and can be validated by a larger sample size with the fine weather conditions in terms of the percentage of procurement of energy.

Keywords: Distributed generation (DG), Fuel cell, Wind turbine, Photovoltaic (PV), Performance analysis

1. Introduction

All technological developments have emerged in line with specific needs. Since the history of humanity, scientists, researchers, engineers, and inventors have been looking for solutions to the problems encountered while working on meeting the needs of people. In response to the problems faced by traditional grids, researchers and scientists have agreed on the need for modernization of the traditional grid. The main problems encountered in traditional grids are transmission losses and energy security due to the transfer of the generated energy to loads that are kilometers away. According to the U.S. Department of Energy, modular, small-scale, on-grid, or off-grid systems, consisting of wind turbines, photovoltaic (PV) modules, hydrogen fuel cells, and energy storage units that provide near-load installation, are called distributed generation (DG) [1]. DG systems are able to continue operating during blackouts, which allows flexible and efficient electrical energy distribution with an integration of renewable energy. DGs are designed for small and medium sized electric power grid to provide energy for dynamic load groups such as organized industrial site, Research & Development centers, university campuses, and technoparks [2].

A lot of definitions are used about DG in the literature. The definition of the nominal values of each distributed power station also differs country wise. Due to the variations when defining DG, the following parameters must be determined: the power location area, the capacity of distributed generation, the used technology, and the operation mode. DG requires efficient and cost-effective integration with the existing grid [3]. It can be presumed that the distributed generation is flexible energy generation system that can operate either connected or independent from the grid, providing installation close to the load groups. This is operated conveniently for flexible and dynamic load groups such as university campuses, educational institutions, and research-development centers.

Although DGs provide flexibility in energy management, the energy production capacities of the wind turbine and PV modules depends largely on meteorological conditions. Therefore, in the absence of sufficient wind and sun, a third support energy generation system is needed. In this study, the hydrogen fuel cell stack was used as a back-up power generation system. The hydrogen used by the fuel cell is produced by the electrolyser operating with the energy produced by using renewable energy sources. This ensures a completely clean and sustainable energy conversion [4]. In this study, unit sizing and performance analysis of the PEMFC based grid-connected distributed generation system at Marmara University, Faculty of Technology, is performed, and analyzed. The rest of the paper is organized as follows: DG Case Studies in World Universities are given briefly. The next section handles the factors need to be set-up for DG system design as Overview of Hybrid Microgrid System. In this Section, each component is examined in detail, their effectiveness is evaluated. For the next one that gives some discussion points about the DG system design, challenges, summarizes regarding operation results. The main points of conclusions remarks are presented in the last section.

2. DG Case Studies at World Universities

One of the best examples of establishing the DG systems on university campuses in the University of California, San Diego (UCSD). The system has installed capacity of 42 MW, and meets 92 % of its annual electricity demands of the UCSD [5].

Fig. 1. The PV modules in UCSD [5].

Another example is the DG system at the Illinois Institute of Technology (IIT). This system includes 4 MW gas turbine, wind turbines, and PV modules [5]. The DG system consists of a 15 MW gas turbine and a 4.5 MW PV plant [6-7].

Fig. 2. Gas-fueled CHP plant in Princeton University.

The DG system installed at Westlakes Campus of Central Lancashire University in England consists of a 5kW wind turbine, a 20 kW PV system, a 21.6 kW heat pump, and a 6 kW solar thermal power system [8]. In addition to these universities, Hangzhou Dianzi University in China, Genoa University in Italy, The University of Nottingham in the UK, Chiang Mai Rajabhat University in Thailand, Technical University of Denmark, and New York University in the USA have small and medium scale capacity DGs [7-12] as can be seen in Fig.1, 2 and 3.

Fig. 3. PV modules and a Micro Turbine in the Genoa University, Savona Campus [10].

3. Overview of Hybrid Microgrid System

The DG system, which is the subject of this study, was established in Marmara University, Faculty of Technology. With this system, university researchers and academicians will be supported in the fields of fuel cell technologies, renewable energy systems, power electronics, sustainable energy management, and hybrid power systems.

Components of the DG system is stated as follows;

- PV modules, 1000 W
- The wind turbine, 400 W
- Hydrogen PEM fuel cell stack, 1200 W
- The hybrid inverter, 2400 W
- The battery bank, 600 Ah, 14.4 kWh
- Fuel cell start-up battery, 2x12V, 120 Ah
- Hydrogen generator (electrolyser), 60sl / h
- Low-pressure hydrogen tank, 1500 sl

• Electronic load, 1500 W
• Central energy management unit.

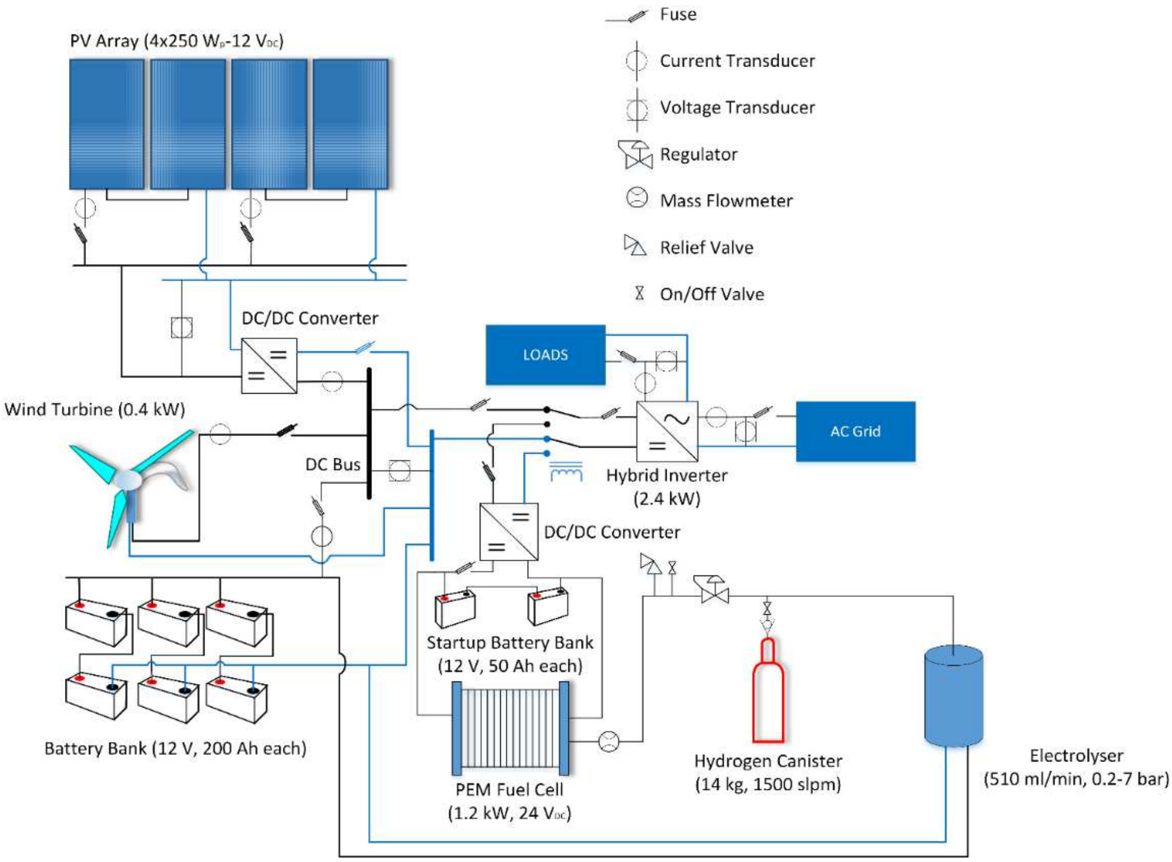

Fig. 4. Overall system diagram.

The monitoring and control part of the DG system consist of two main parts: energy production and energy storage. Energy production units comprise of a wind turbine, photovoltaic modules, and proton exchange membrane fuel cell (PEMFC) system. The storage part consists of a battery bank, hydrogen canister, and electrolyser. PEM type hydrogen fuel cell is used as a backup energy generation system in this hybrid DG structure. Since the polymer material is used as the electrolyte in the hydrogen fuel cell, these fuel cells are called "Proton Exchange Membrane" (PEM). The electrodes used are carbon structured. The most important feature of the PEMFC is that it has a membrane with proton conduction. The polymer membrane used is thin, small, and light. The most commonly used membrane material is Nafion®, manufactured by DuPont. This membrane must be made of a material with high thermal, mechanical, and chemical resistance that is impermeable to water, fuel, oxygen, and other gases in the air. The wind turbine and photovoltaic modules on the rooftop of the Marmara University, Faculty of Technology, are shown in Fig. 5. The laboratory room where the wind turbine, photovoltaic modules are connected, the stack of hydrogen fuel cells, the battery bank, the electrolyser, the hydrogen canister, and other components can be seen in Fig. 6.

Fig. 5. Wind turbine and photovoltaic modules on the rooftop of the faculty building.

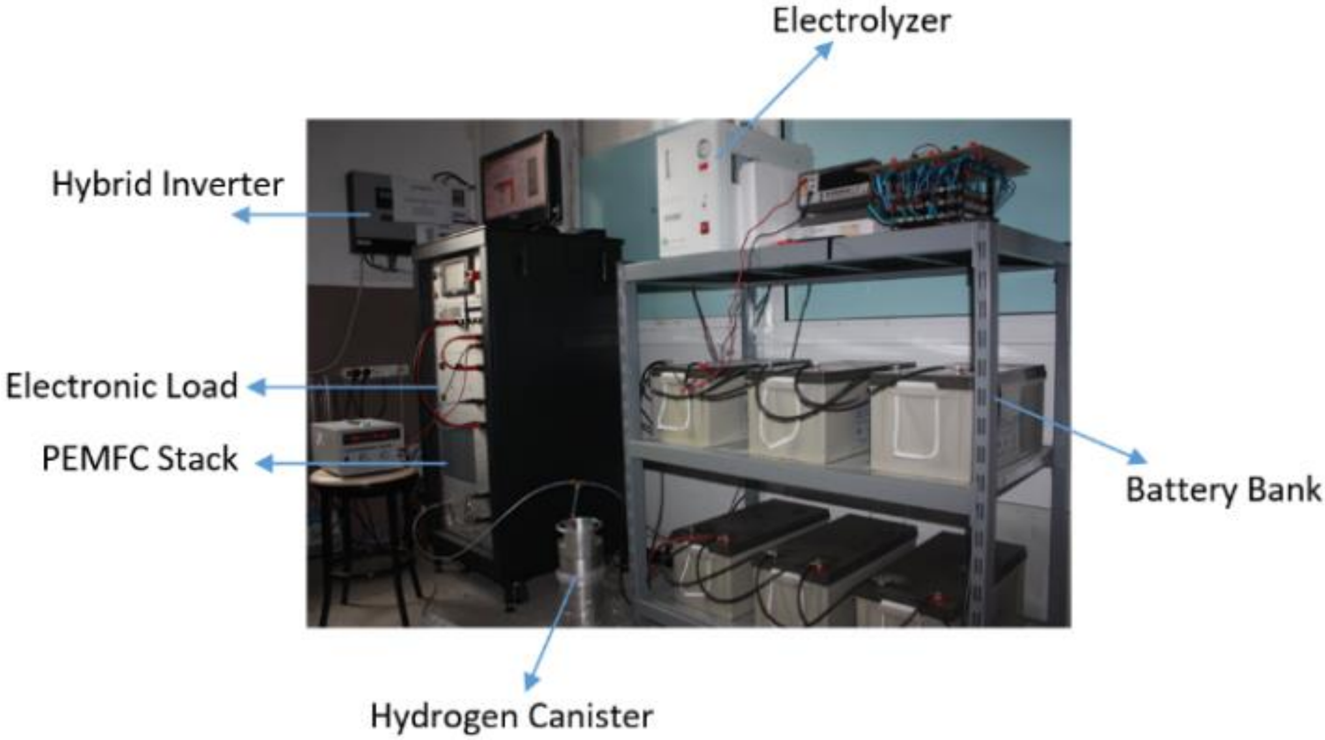

Fig. 6. The DG system components.

Beginning from the wind turbine, the performance analysis of the system components is performed. Also, the wind turbine specifications exist in Table 1.

Table 1. Wind Turbine Specifications.

Specifications	Unit
Nominal Power	400 W
Swept Area	1.07 m^2
Cut-in wind speed	3.58 m/s
Cut-off wind speed	49.2 m/s
Rotor diameter	1.17 m
Alternator	Permanent Magnet Brushless

The Weibull probability density function is usually used to calculate the energy generated from the wind turbine depending on the momentarily variable wind.

$$f(v) = \frac{k}{c}\left(\frac{v}{c}\right)^{k-1} exp\left[-\left(\frac{v}{c}\right)^{k}\right] \tag{1}$$

Where; k is called the shape parameter, and c is called the scale parameter. In those cases, too much detail is known about the wind regime in a region, the k shape parameter can be set to 2. In that case, the Weibull probability density function is called the Rayleigh probability density function [13-14].

$$f(v) = \frac{2v}{c^2} exp\left[-\left(\frac{v}{c}\right)^{2}\right] \tag{2}$$

$$f(v) = \frac{\pi v}{2\bar{v}^2} exp\left[-\frac{\pi}{4}\left(\frac{v}{\bar{v}}\right)^{2}\right] \tag{3}$$

$\bar{v}$ =Average wind speed (m/s) =4.78 m/s

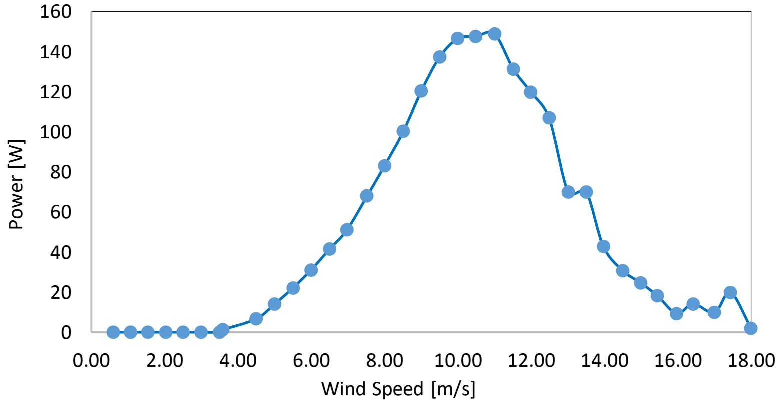

Fig. 7. Power curve of wind turbine.

According to the Weibull calculations, the wind turbine power curve can be expressed in Fig. 7. The total annual obtained energy from the wind turbine is calculated as 228.493 kWh as seen in Table 2.

Table 2. Rayleigh probability density functions and wind turbine calculations.

Wind Speed [m/s]	**Power [W]**	$f(v)$	**Hours/year at v**	**Energy [Wh/year]**
1.06	0	0.065	569.4	0
2.02	0	0.1194	1045.944	0
2.99	0	0.1512	1324.512	0
3.58	1	0.1581	1384.956	1620.39852
5.00	14	0.1453	1272.828	17921.41824
5.99	31	0.1196	1047.696	32499.52992
6.97	51	0.0893	782.268	39848.73192
8.00	83	0.0609	533.484	44311.18104
9.00	120	0.0382	334.632	40232.80536
10.00	146	0.0221	193.596	28357.94208
11.00	149	0.0118	103.368	15372.88896
11.99	120	0.00585	51.246	6140.80818

13.01	70	0.00268	23.4768	1643.376
13.97	43	0.00114	9.9864	427.817376
14.99	25	0.000452	3.95952	97.4833824
15.97	9	0.000166	1.45416	13.5091464
17.00	10	0.0000569	0.498444	4.8847512
18.00	2	0.000018	0.15768	0.3169368
			Total	228493.0918

Table 3. PV module (polycrystalline cells) specifications.

Features	Values (UOM)
Module Efficiency (%)	15.71
Cell Efficiency (%)	17.9
Peak Power	250 Wp
Max Power Voltage (Vmp)	30.6V
Max Power Current (Imp)	8.17A
Open Circuit Voltage (Voc)	38 V
Short Circuit Current (Isc)	8.71A
Number of Cell	60
Dimensions	1640x990x35 mm

The parameters of the PV module are reported in Table 3. With regards to geographic location, the coordinates of the aforementioned the system are on 40°59′ North Latitude, 29°3′ East Longitude.

$$\delta = 23.45 \sin\left[\frac{360}{365}(n-81)\right] \tag{4}$$

$$\beta_A = 90 - L + \delta \tag{5}$$

$$PV_{tilt} = 90 - \beta_A \tag{6}$$

Where; δ is solar declination angle, β_A is an altitude angle, the altitude angle is the angle between the sun and the local horizon directly beneath the sun. Besides, PV_{tilt} is optimum PV module tilt angle= 30º fixed, *L is* the latitude of the site and *n* is number of day.

$$I_{total} = I_{beam} + I_{diffuse} + I_{reflected} \tag{7}$$

$$I_{beam} = I_{BH} R_B \tag{8}$$

$$I_{BH} = I_H - I_{DH} \tag{9}$$

$$R_B = \frac{\cos(L-PV_{tilt})\cos\delta\sin H_{SRC} + H_{SRC}\sin(L-PV_{tilt})\sin\delta}{\cos L\cos\delta\sin H_{SR} + H_{SR}\sin L\sin\delta} \tag{10}$$

$$H_{SR} = \cos^{-1}(-\tan L \tan\delta) \tag{11}$$

$$H_{SRC} = min\{\cos^{-1}(-\tan L\tan\delta), \cos^{-1}[-\tan(L - PV_{tilt})\tan\delta]\} \tag{12}$$

$$C = \frac{I_H}{I_O} \tag{13}$$

$$\frac{I_{DH}}{I_H} = 1.390 - 4.207C + 5.531C^2 - 3.108C^3 \tag{14}$$

$$I_{diffuse} = I_{DH}\left(\frac{1+\cos(PV_{tilt})}{2}\right) \tag{15}$$

$$I_O = \left(\frac{24}{\pi}\right) SC\left[1 + 0.034\cos\left(\frac{360n}{365}\right)\right](\cos L \cos\delta \sin H_{SR} + H_{SR}\sin L \sin\delta) \tag{16}$$

$$I_{reflected} = \rho I_H\left(\frac{1-\cos(PV_{tilt})}{2}\right) \tag{17}$$

Where; I_{total} is total daily solar irradiance on the PV module, I_{beam} is beam solar irradiance on the PV module, $I_{diffuse}$ is diffuse solar irradiance on the PV module, $I_{reflected}$ is reflected solar radiation on the PV module, I_H is total average daily horizontal solar irradiance, I_{BH} is beam irradiance on the horizontal surface, R_B is beam tilt factor, H_{SRC} is the sunrise hour angle for the collector (when the sun first strikes the collector face, θ = 90°). And H_{SR} is the sunrise hour angle (in radians), C is clearness index, I_O is extraterrestrial insolation on a horizontal surface the site, $I_H$is insolation on a horizontal surface, lastly ρ is ground reflectivity. The total solar irradiance profile can be stated in Fig. 8.

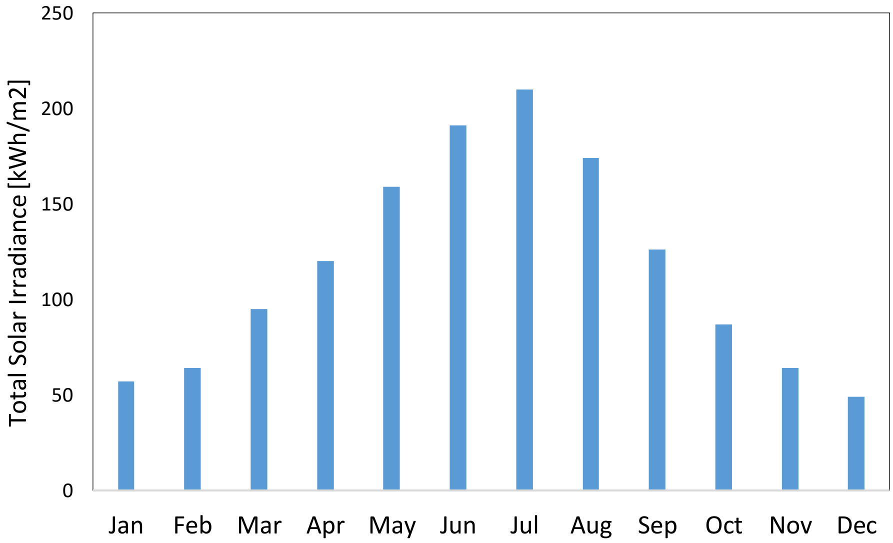

Fig. 8. Monthly solar irradiance.

The 3DSun-Path program has been used to assist in comparing solar altitude, azimuth angles, and zenith angles. The program interface is shown in Fig. 9.

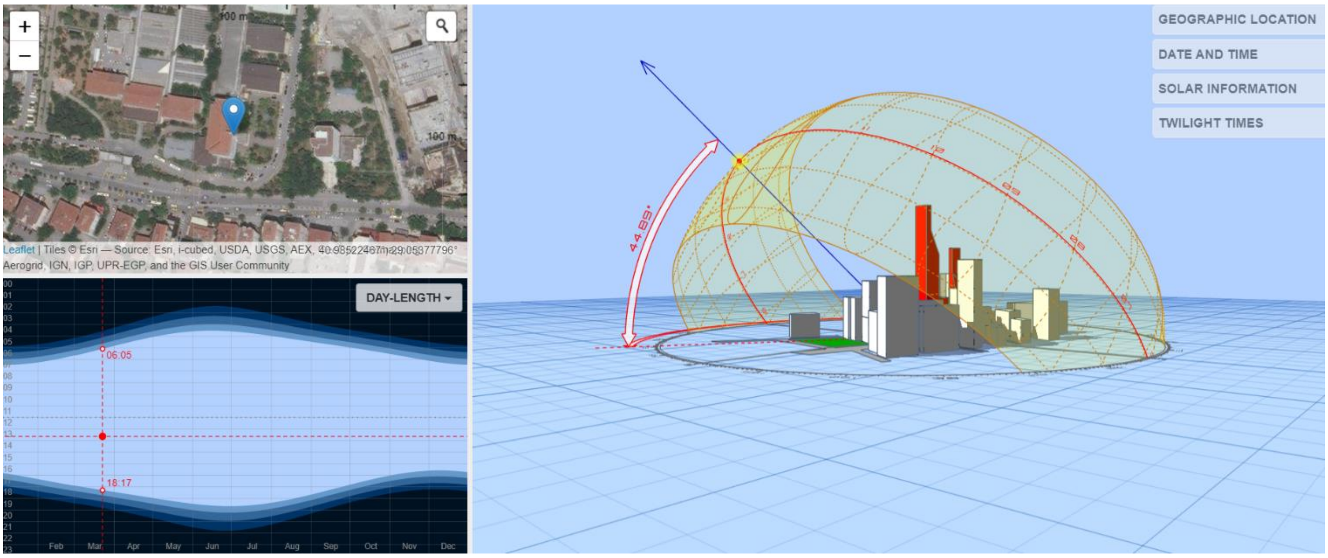

Fig. 9. Geographic location of the faculty building and solar positions [15]

$$E_{total} = A_{module}.\eta_{module}.I_{total}.PR \tag{18}$$

E_{total} is produced Total PV output energy (kWh), PR is performance ratio (0.5~0.9), A_{module} is module area (m^2), and η_{module} is module efficiency (%).

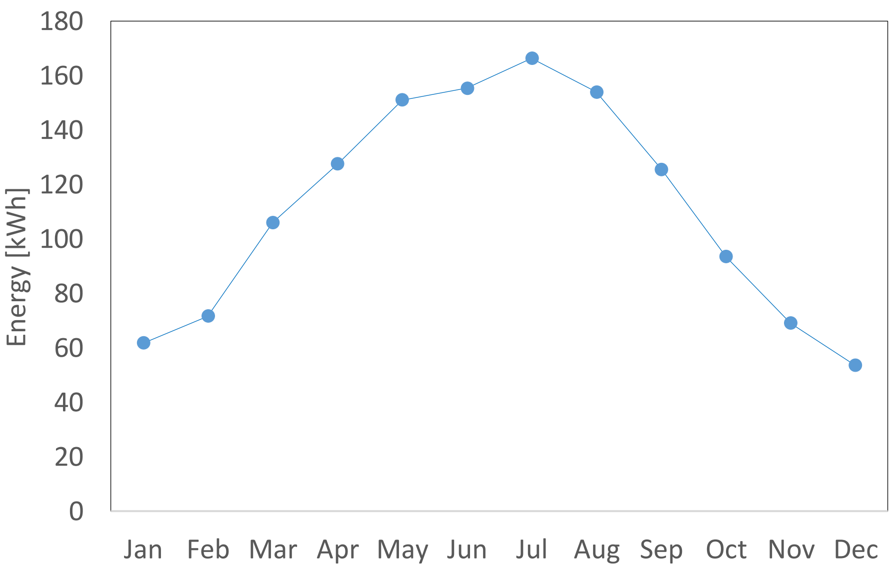

Fig. 10. Produced PV total output energy.

Equation (18) expresses total annual produced PV energy. By this calculation, the annual average produced energy profile is plotted and illustrated in Fig. 10, also annual total PV energy corresponds 1335.05 kWh. Fig. 11 depicts the hourly total produced PV output energy. It can be extracted that generation is higher at noon times than the other times when the energy extracts.

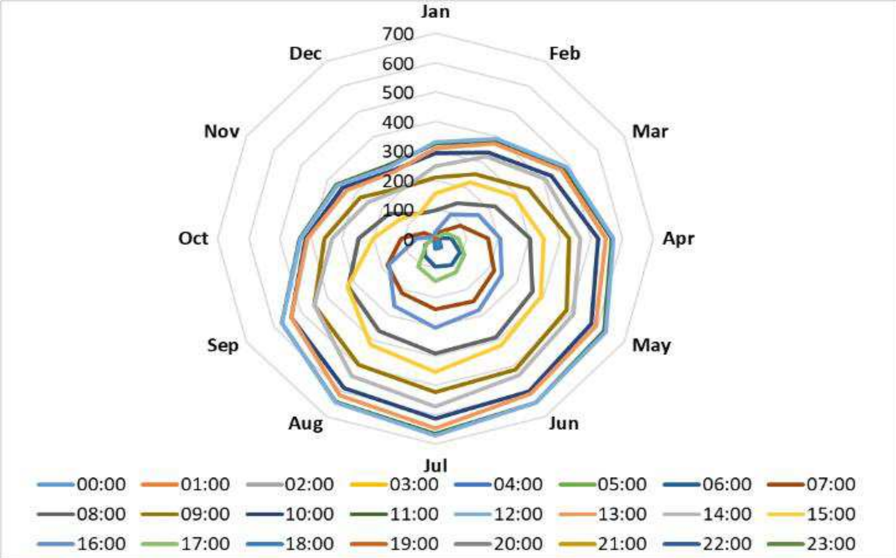

Fig. 11. Hourly total produced PV output energy [kWh].

The system is designed to operate both independently and connected to the grid. The system can be connected to the grid via hybrid inverter when the battery bank where the generated energy is stored cannot meet the load requirement. When the battery bank meets the load requirement, the system operates independently of the grid.

Table 4. The load profile of the laboratory.

Loads	**#**	**Nominal Power [W]**	**Hours of use/day**	**Energy use/day [Wh/day]**
Air Conditioning	1	560	5*	2800
Electrolyser	1	400	2	800
Lighting	12	48	10*	5.760
PC	2	250	10	5000
Total		2.616		14360

*Discrete time

As seen in Table IV, the daily energy requirement was calculated as 14,360 kWh. In this case, the annual average energy demand is 3791.04 kWh. Since the total annual energy demand is 3791.04 kWh, 2029.497 kWh of energy which cannot be met by production can be supplied from the grid via hybrid inverter.

$$Ah = \frac{n.k.E_{demand}}{V_{DC}.\text{DoD}} \tag{19}$$

Where; n is days of autonomy (n = 2), DOD is maximum depth of discharge (DoD = 40%), V_{DC} is DC bus voltage (V_{DC} = 24 V), E_{demand} is total energy demand, k is temperature Correction Factor (k = 1.04). On the other hand, six pieces of batteries of 120 Ah each are connected in series and parallel as shown in Fig. 5 to get 24 V nominal and a total power of 14.4 kWh. The system components are installed in "Renewable Energy Laboratory" within the Faculty. The lighting armatures and the "plug and play" loads connected to the DG system. The lighting loads are shown in Fig. 12.

Fig. 12. The lighting loads in the laboratory.

The annual average energy produced from wind turbine and photovoltaic modules is 1563.543 kWh. The PEMFC can generate 198 kWh of energy per year when we estimate that it produces 3 hours of average power per day. In this case, the total energy produced from the hybrid micro grid is 1761.543 kWh. By means of the electrolyser in the system, the hydrogen demand of the hydrogen fuel cell stack can be met. The hydrogen produced by the electrolyser is stored in the metal hydride canister. The charge pressure of the metal hydride canister is 5 bar and the discharge pressure is between 2-5 bar. Weight is 14 kg and capacity is 1500 lt. The empty canister can be fully filled in 50 hours. PEM type hydrogen fuel cell stack is used in the system. The stack in the system can run for 8 hours with a full hydrogen canister at 250 W average. In order for the hydrogen fuel cell stack to operate at a maximum power of 1200 W, it should be supplied with 13 liters of hydrogen per minute. The output flow of the electrolyser used in the system is 510 ml per minute. Therefore, the produced hydrogen should be stored in order for the heap to operate at a power of 300 W.

A Graphical User Interface (GUI) is used for the hydrogen fuel cell stack used in the system, as shown in Fig. 13. With the help of this interface, all inputs and outputs of the system can be monitored and controlled in real time.

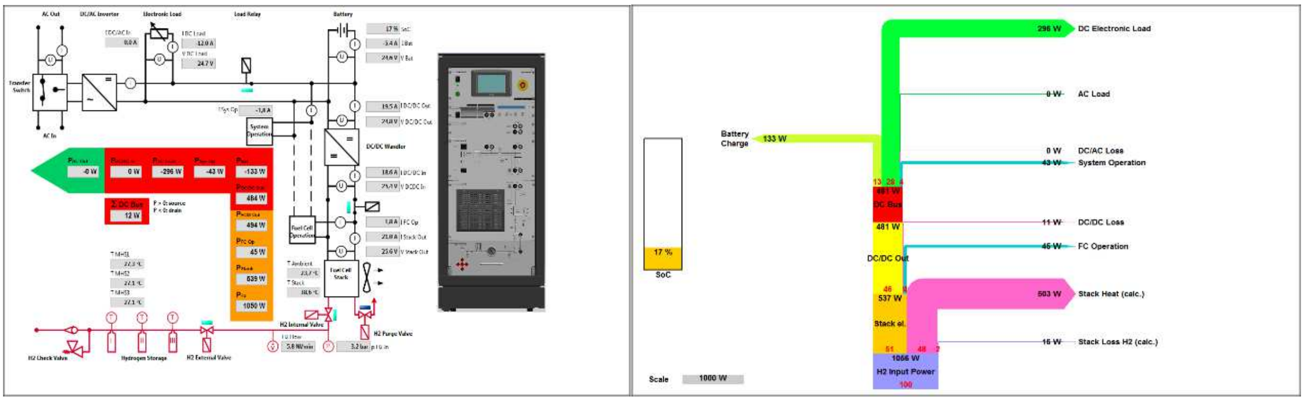

Fig. 13. GUI PEMFC Stack,components and sankey diagram

Additionally, polarization curves of fuel cells for different load characteristics, determination of charge-discharge characteristics of batteries, energy conversion and efficiency analysis, wind turbine and photovoltaic module data were obtained. The input power of the system, the powers used and the energy losses are shown in a Sankey diagram. This diagram also shows the state of charge of the start-up batteries of the fuel cell stack as can be seen in Fig. 13. The most important parameter of a hydrogen fuel cell is the polarization curve. The polarization curve is a graph showing the change in current of a fuel cell or stack depending on voltage or power. This curve determines the performance of the cell. Through the GUI it is possible to monitor the instantaneous polarization curve of PEMFC Stack can be shown in Fig. 14.

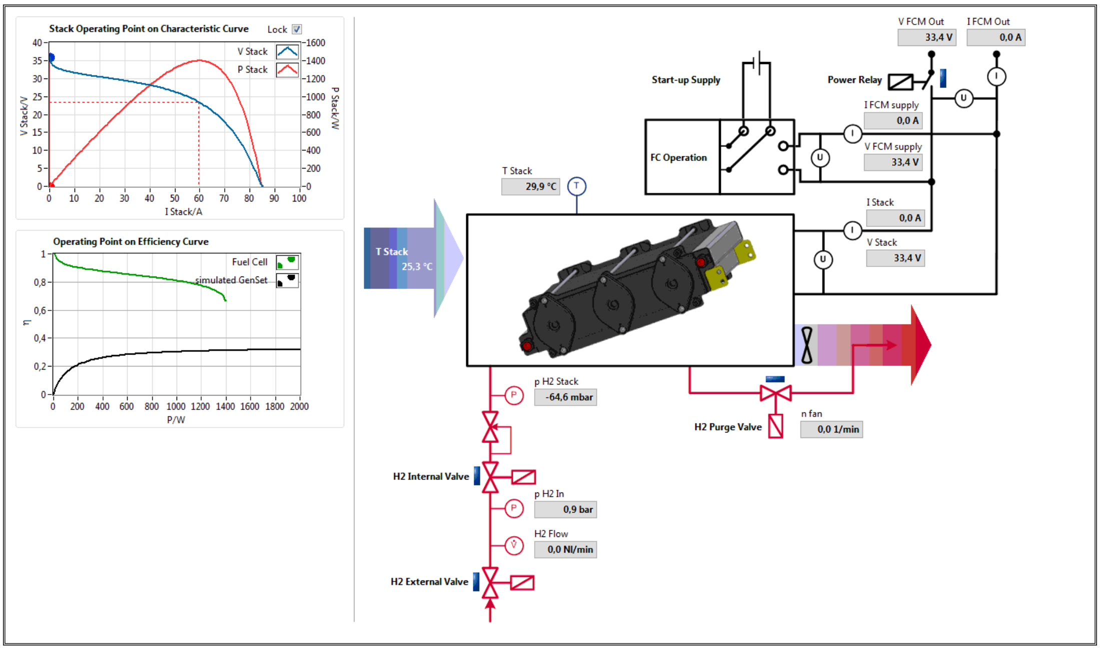

Fig. 14. The Polarization Curves of The PEMFC.

The GUI of the PEMFC monetarizes and also facilitates data acquisition relevant to all variables are also seen in Fig. 15.

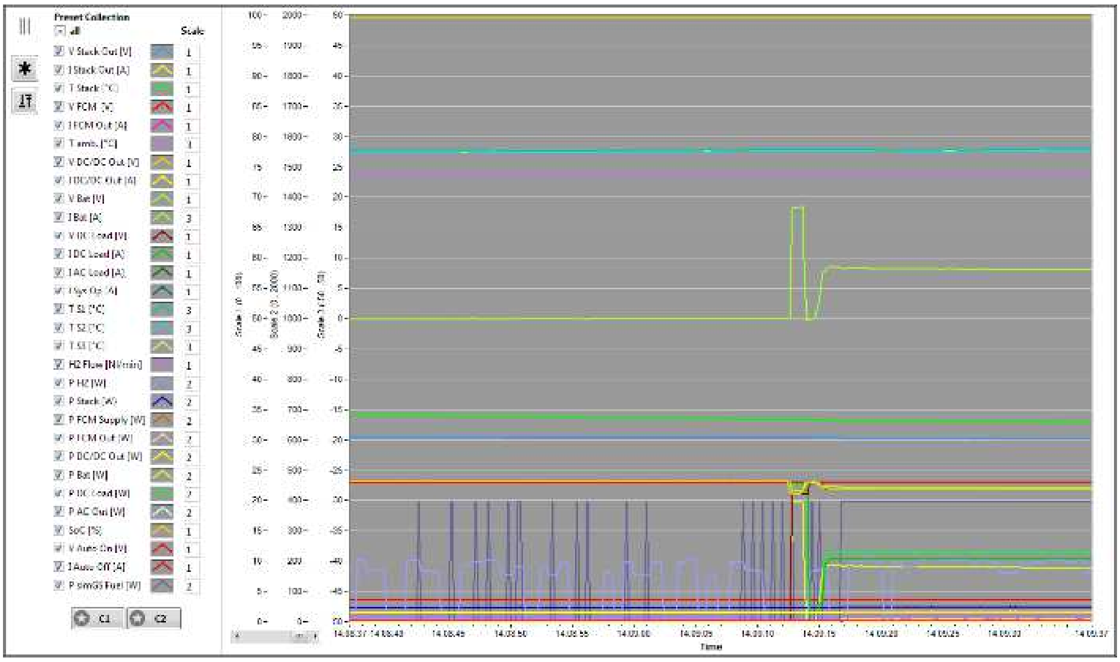

Fig. 15. Data acquisition screen.

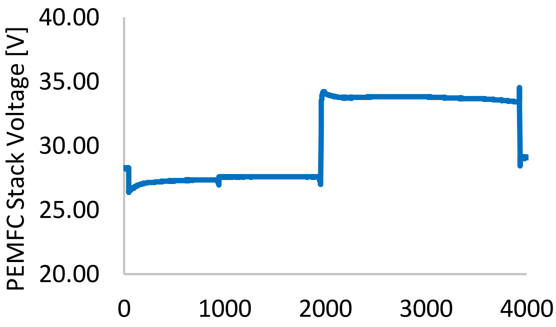

a)

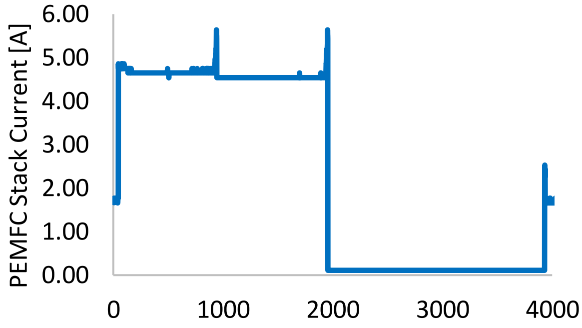

b)

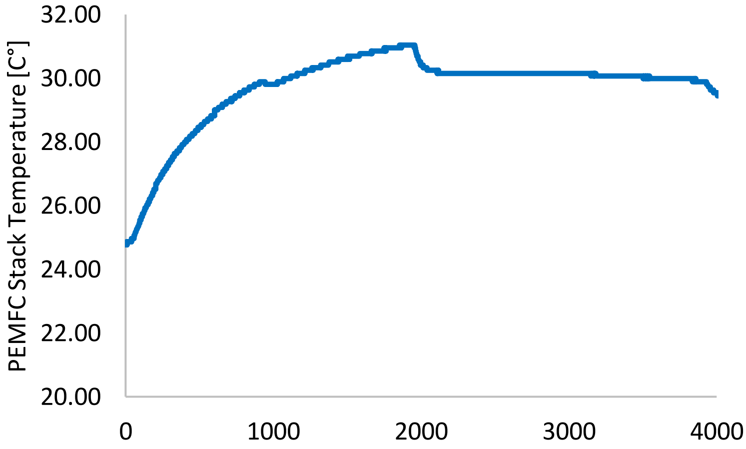

c)

Fig. 16. a) PEMFC stack voltage, b) PEMFC stack current, c) PEMFC stack temperature [C°].

Fig. 16 shows the voltage, current, power and temperature curves of the collected PEMFC stack for approximately one hour (4000 seconds). Besides, the data for the SoC level of the start-up battery and PEMFC's DC/DC converter output voltages, were drawn by collecting in Fig.17.

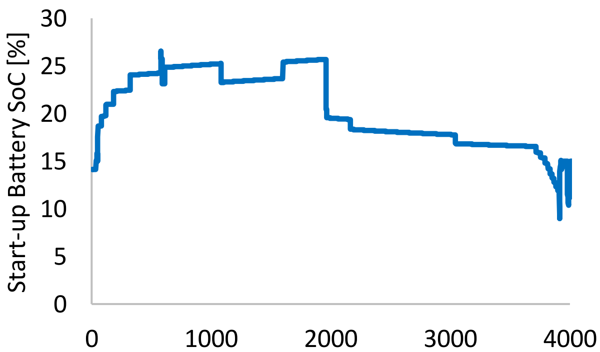

a)

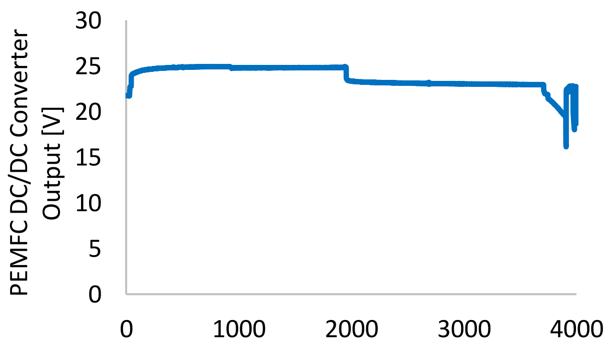

b)

Fig. 17. a) Start-up battery state of charge (SoC) levels, b) PEMFC's DC/DC converter output voltages

4. Operation Results

The PEMFC based grid-connected DG system at Marmara University, Faculty of Technology was analyzed in detail in this study. 53.53% of the total energy demand is met by the utility grid, while 46.47% of the demand is met by the DG system as can be seen in Fig. 18.

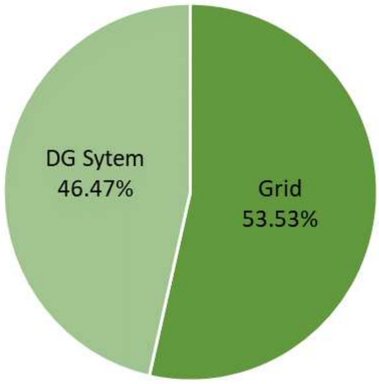

Fig. 18. Grid support and DG energy produce.

Energy supplied from the utility grid, production of DG systems and energy demands for the system are given in Table 5. With respect to the energy values of DGs as kWh, most of the demands are met by PV as 35.22% of total produce i.e., nearly 76% among DGs as can be seen in Fig. 19. The contribution of the wind and PEMFC i.e., the rest of PV (nearly 24% among DGs) has almost close percentages as 6.02% and 5.23%, respectively.

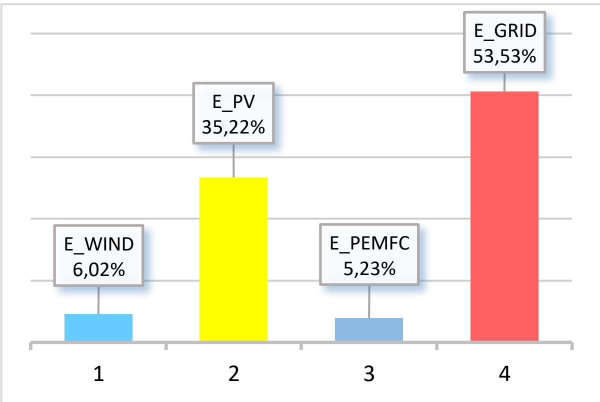

Fig. 19. The pie chart of power generation and grid support rates of the microgrid for a defined operation.

Table 5. The distributed generation and energy demands [kWh].

E_{Wind}	E_{PV}	E_{PEMFC}	E_{demand}	E_{grid}
228.493	1335.05	198	3791.04	2029.497

5. Conclusion

According to the results of the performance analysis, the important points that will be highlighted and will help the researchers working in this field are as follows. First of all, it can be extracted that the PV modules are more useful and efficient in urban applications than wind turbines. For example, we can hardly see 160 W of a wind turbine with a nominal 400 W of power used in this system. The most important reason for this is that the wind turbines installed in places where there are many buildings cannot catch the necessary wind due to the dynamic nature of the wind. Another important consequence of the DG system is that the hydrogen required by the fuel cell is supplied by the electrolyser which is supplied from renewable energy instead of ready hydrogen tanks. However, the PEM type fuel cell stack is not suitable for continuous operation if the electrolyser has a low hydrogen producing capacity. Although the nominal power of the fuel cell is 1200 W, it is operated with 250 W output power. The energy required for the operation of electrolyser is produced entirely from renewable energy. With the increase of the power and size of the electrolyser, PEMFC's support for the DG system will increase even more.

The key components of the system are power switching and power electronics components. The frequency of the power switching elements of the inverter used in the system during connection and disconnection from the grid affects the loads in the system. This particularly affects fluorescent luminaires, which operate with a gas discharge.

Acknowledgement

This study was supported by grant from Scientific Research Projects Unit (BAPKO) project number: FEN-E-120314-0069.

Authors' contributions

ANA and ED wrote the manuscript. ED performed the experimental design of this microgrid and data acquisition. ANA operated the system. ANA and ED gathered and evaluated the results. ANA and ED reviewed the manuscript. All authors read and approved the final manuscript.

Funding

This research did not receive any specific grant from funding agencies in the public, commercial, or not-for-profit sectors.

Availability of data and materials

Not applicable.

Ethics approval and consent to participate

Not applicable.

Consent for publication

Not applicable.

Competing interests

The authors declare that they have no competing interests.

Author details

[1]Department of Electrical-Electronics Engineering, Faculty of Technology, Marmara University, Istanbul, Turkey

References

[1] About Microgrids, Microgrids at Berkeley Lab. https://building-microgrid.lbl.gov/about-microgrids, [accessed 15 May 2020].

[2] Unamuno E, Barrena JA. Hybrid AC/DC microgrids—Part I: Review and classification of topologies. Renew Sust Energ Rev 2015;52:1251-1259. https://doi.org/10.1016/j.rser.2015.07.194.

[3] U.S. Department of Energy. Distributed Energy. Retrieved from http://energy.gov/oe/technology-development/smart-grid/distributed-energy [accessed 16 May 2020].

[4] Leto S, Sun C. A novel joint bidding technique for fuel cell wind turbine photovoltaic storage unit and demand response considering prediction models analysis Effect's. Int J Hydrog Energy 2020; 45:6823-6837. https://doi.org/10.1016/j.ijhydene.2019.12.210

[5] Han Y, Chen W, Li Q, Yang H, Zare F, Zheng Y. Two-level energy management strategy for PV-Fuel cell-battery-based DC microgrid. Int J Hydrog Energy 2019;44:19395-19404. https://doi.org/10.1016/j.ijhydene.2018.04.013

[6] Washom B, Dilliot J, Weil D, Kleissl J, Balac N, Torre W, Richter C. Ivory Tower of Power: Microgrid Implementation at the University of California, San Diego. IEEE Power Energy M 2013;11:28-32. https://doi.org/10.1109/MPE.2013.2258278

[7] Liang C, Shahidehpour M, DC Microgrids: Economic Operation and Enhancement of Resilience by Hierarchical Control. IEEE T Smart Grid 2014;5:2517–2526.

[8] Case study: Microgrid at Princeton University, Consulting-Specifying Engineer, 2015. http://www.csemag.com/single-article/case-study-microgrid-at-princeton university/a852c6c36420f738c8ecf66de7aa3dd1.html [accessed 20 May 2020].
[9] The University of Central Lancashire (UCLAN) http://www.uclan.ac.uk/courses/msc_pgdip_renewable_energy_engineering.php [accessed 20 May 2020].
[10] The Microgrids Group at Berkeley Lab, "Examples of Microgrids", Berkeley Lab., 2019. https://building-microgrid.lbl.gov/examples-microgrids [accessed 20 May 2020].
[11] Bracco S, Delfino F, Pampararo F, Robba M, Rossi M. Planning and management of sustainable microgrids: The test-bed facilities at the University of Genoa. 2013 Africon, Pointe-Aux-Piments, 2013:1-5. https://doi.org/10.1109/AFRCON.2013.6757862
[12] Davies R, Sumner M, Christopher E. Energy storage control for a small community microgrid. 7th IET International Conference on Power Electronics, Machines and Drives (PEMD 2014), Manchester, 2014:1-6. https://doi.org/10.1049/cp.2014.0508
[13] Setthapun W, Srikaew S, Rakwichian J, Tantranont N, Rakwichian W, Singh R. The integration and transition to a DC based community: A case study of the Smart Community in Chiang Mai World Green City. 2015 IEEE First International Conference on DC Microgrids (ICDCM), Atlanta, GA, 2015:205-209. https://doi.org/10.1109/ICDCM.2015.7152039
[14] Masters GM. Renewable and Efficient Electric Power Systems, IEEE Press and Wiley; 2014.
[15] Mihet-Popa L, Groza V, Isleifsson F. Experimental testing for stability analysis of distributed energy resources components with storage devices and loads. 2012 IEEE International Instrumentation and Measurement Technology Conference Proceedings, Graz, 2012:588-593.
[16] Dr. Andrew Marsh, 3D Sun-Path, https://drajmarsh.bitbucket.io/sunpath3d.html [accessed 01 June 2020].

Figures

Figure 1

The PV modules in UCSD [5].

Figure 2

Gas-fueled CHP plant in Princeton University.

Figure 3

PV modules and a Micro Turbine in the Genoa University, Savona Campus [10].

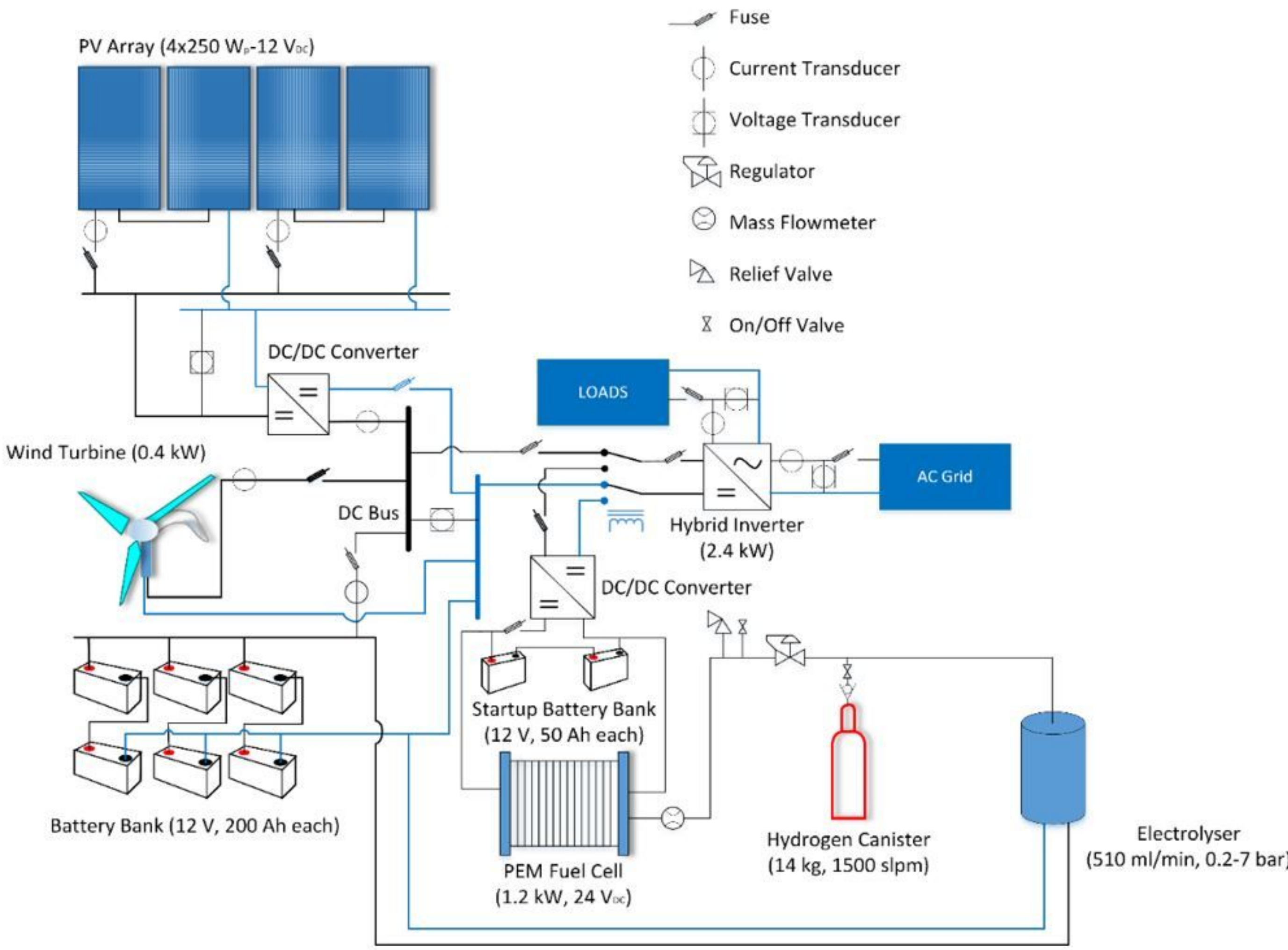

Figure 4

Overall system diagram.

Figure 5

Wind turbine and photovoltaic modules on the rooftop of the faculty building.

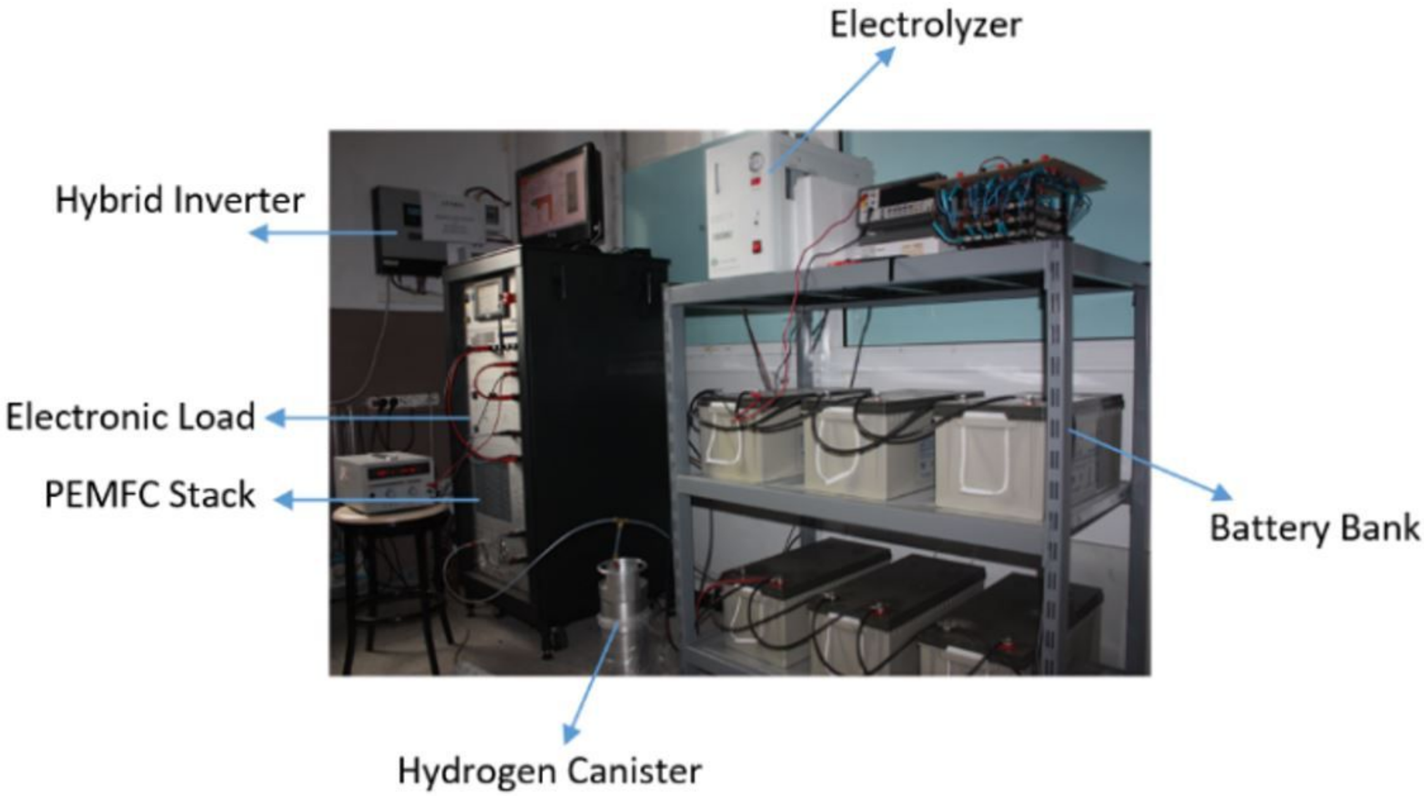

Figure 6

The DG system components.

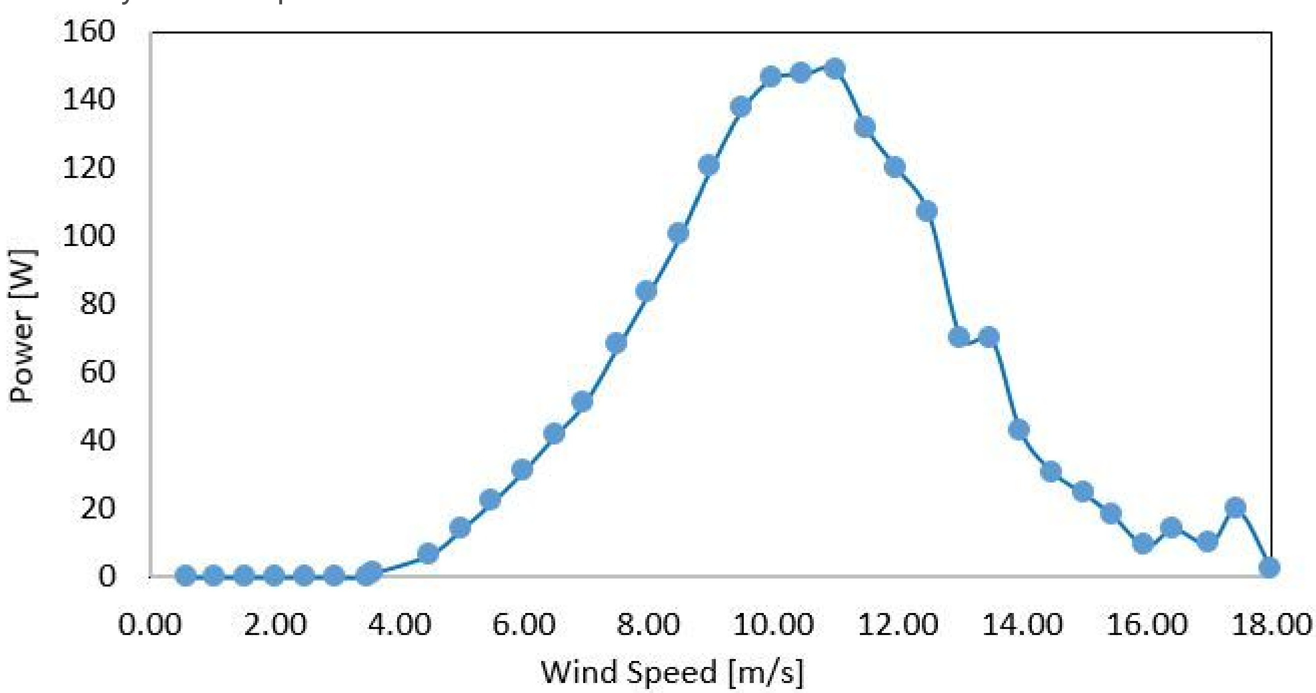

Figure 7

Power curve of wind turbine.

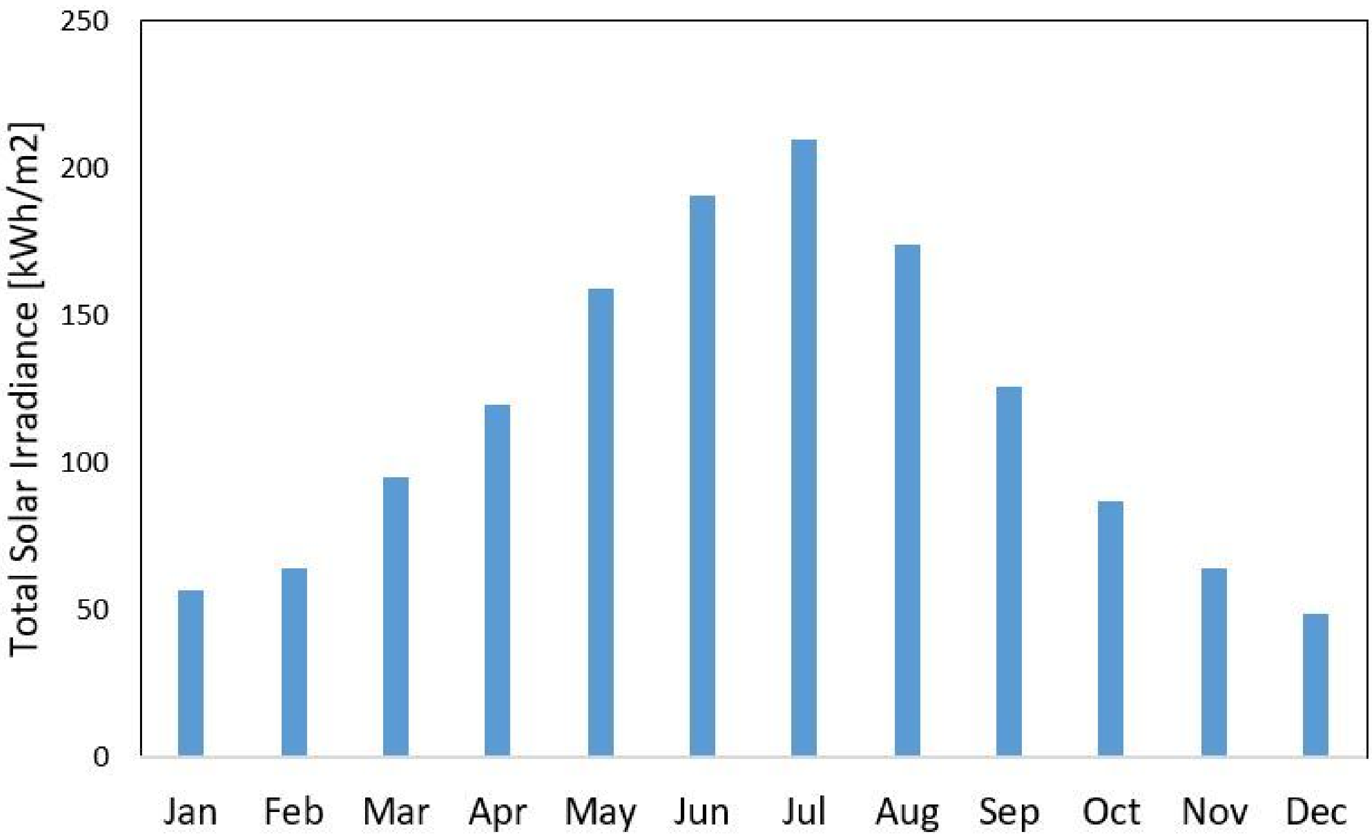

Figure 8

Monthly solar irradiance.

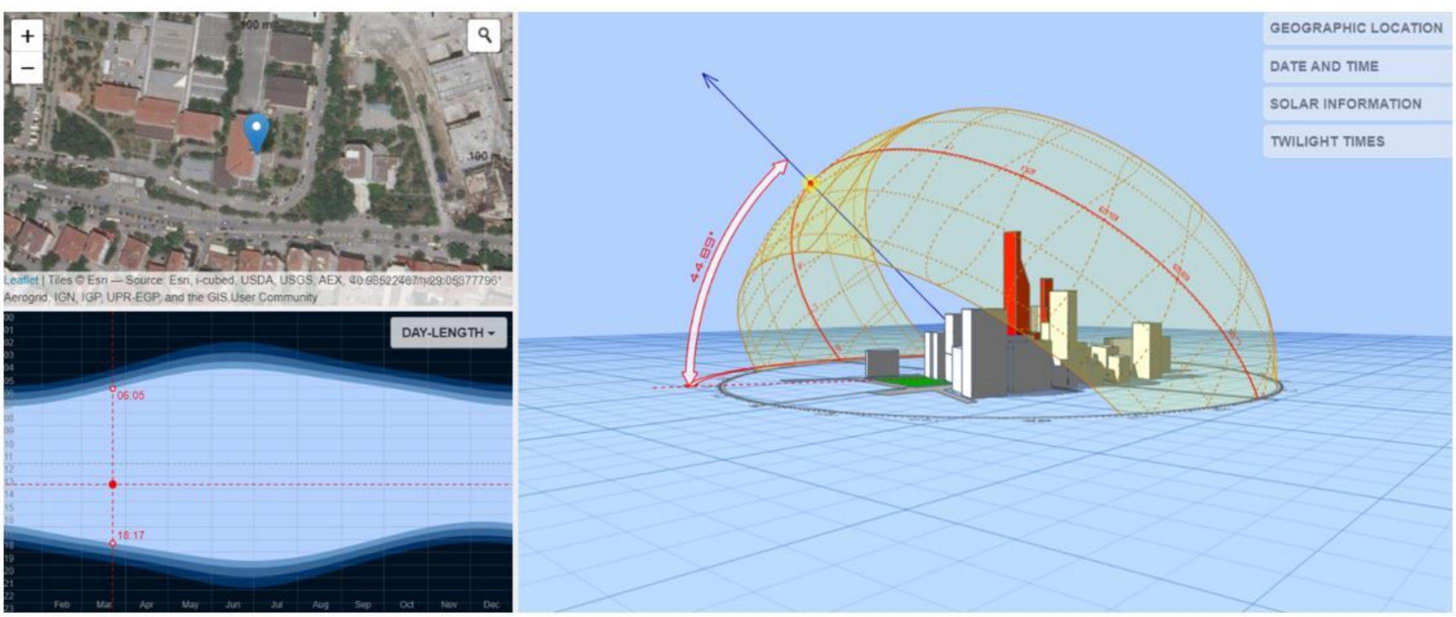

Figure 9

Geographic location of the faculty building and solar positions [15]

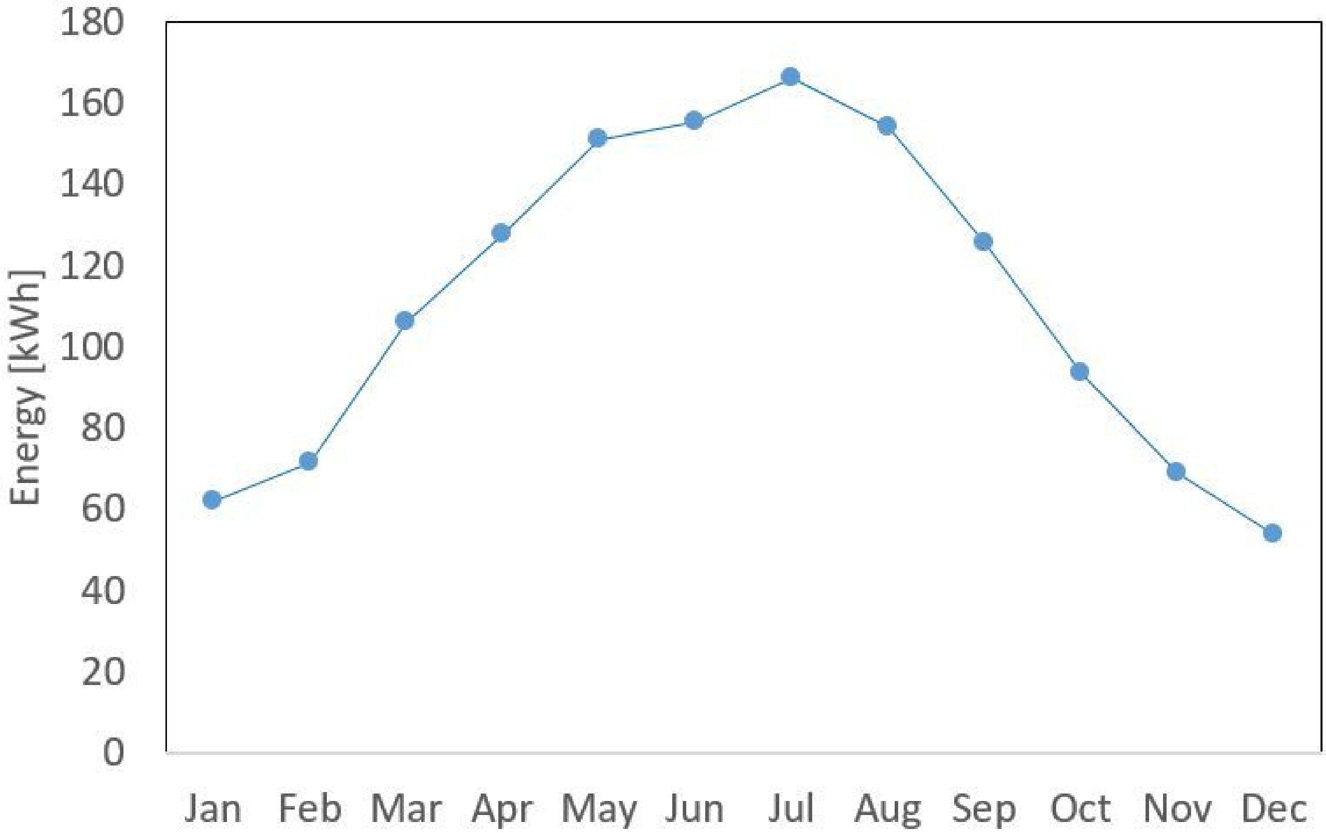

Figure 10

Produced PV total output energy.

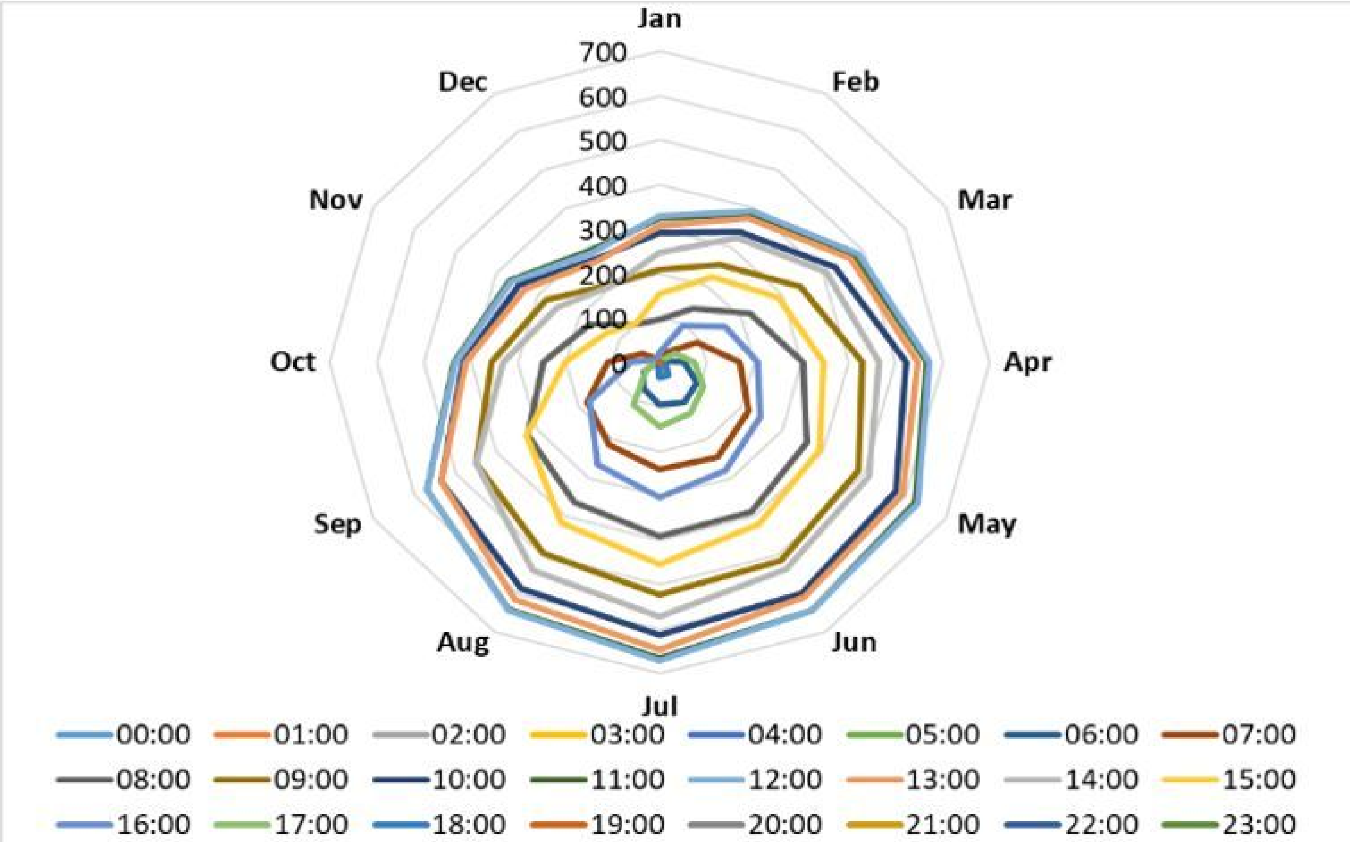

Figure 11

Hourly total produced PV output energy [kWh].

Figure 12

The lighting loads in the laboratory.

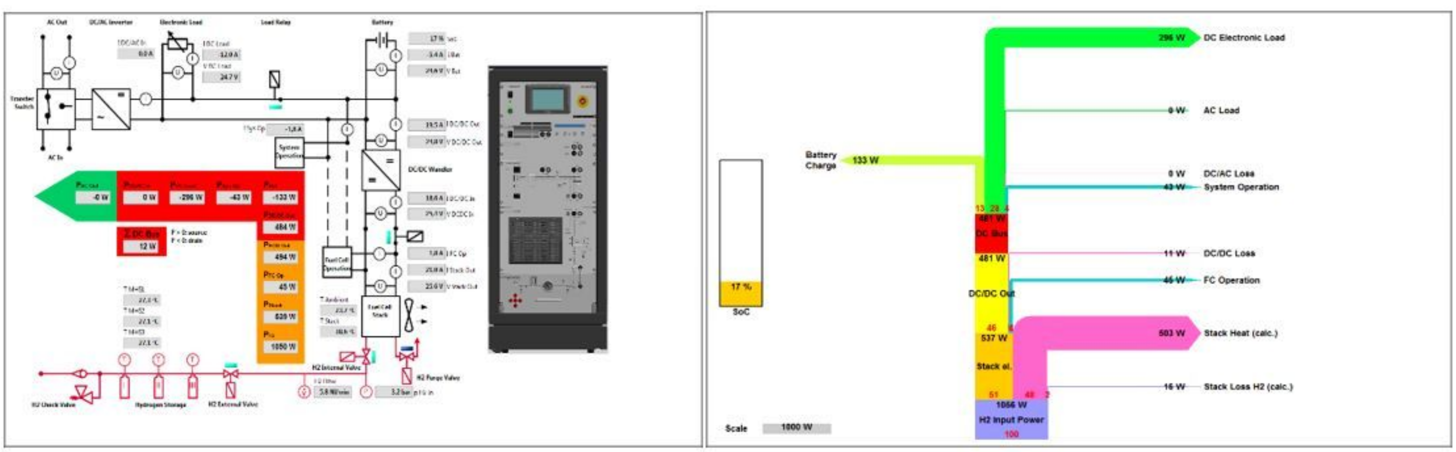

Figure 13

GUI PEMFC Stack,components and sankey diagram

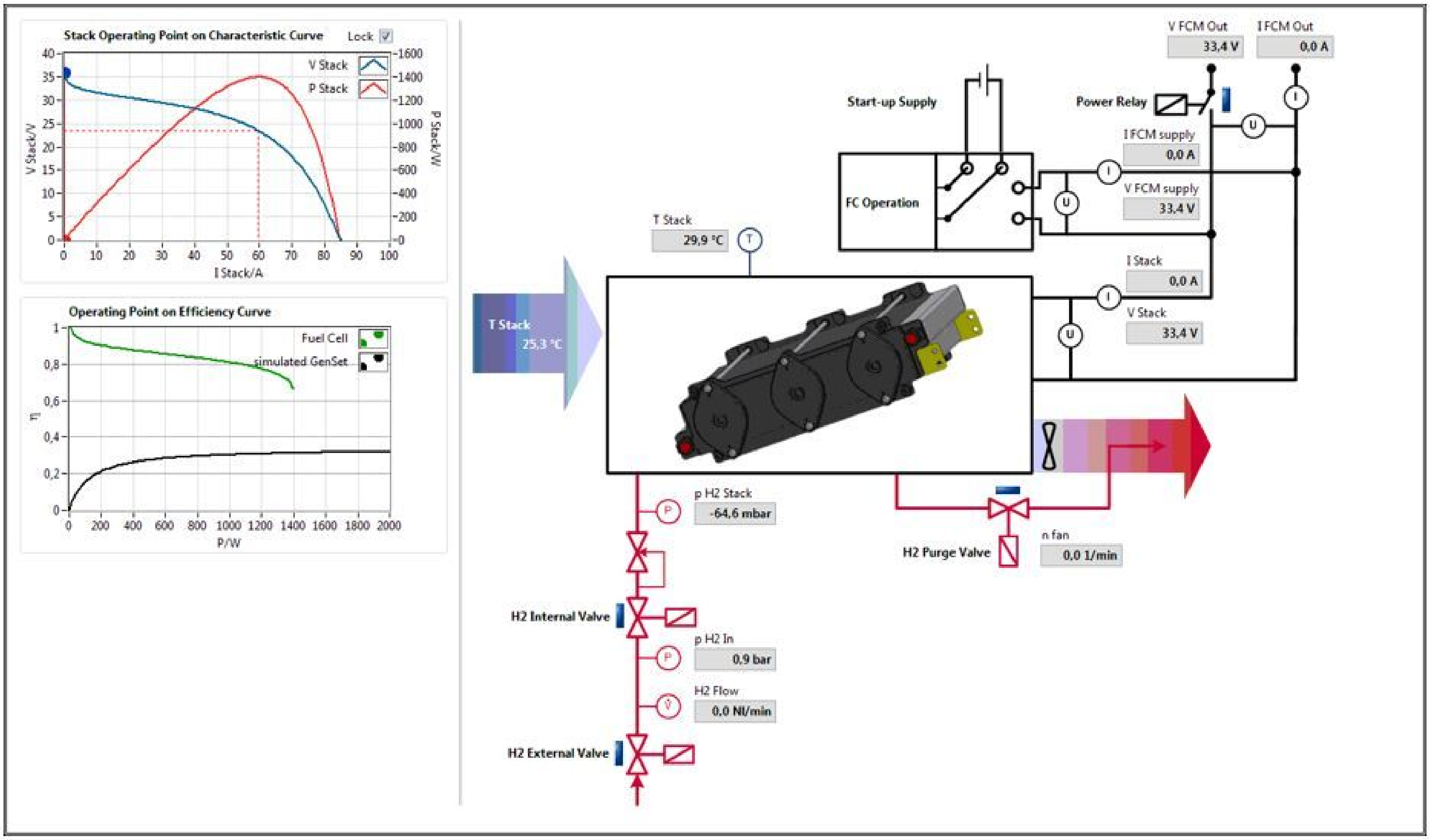

Figure 14

The Polarization Curves of The PEMFC.

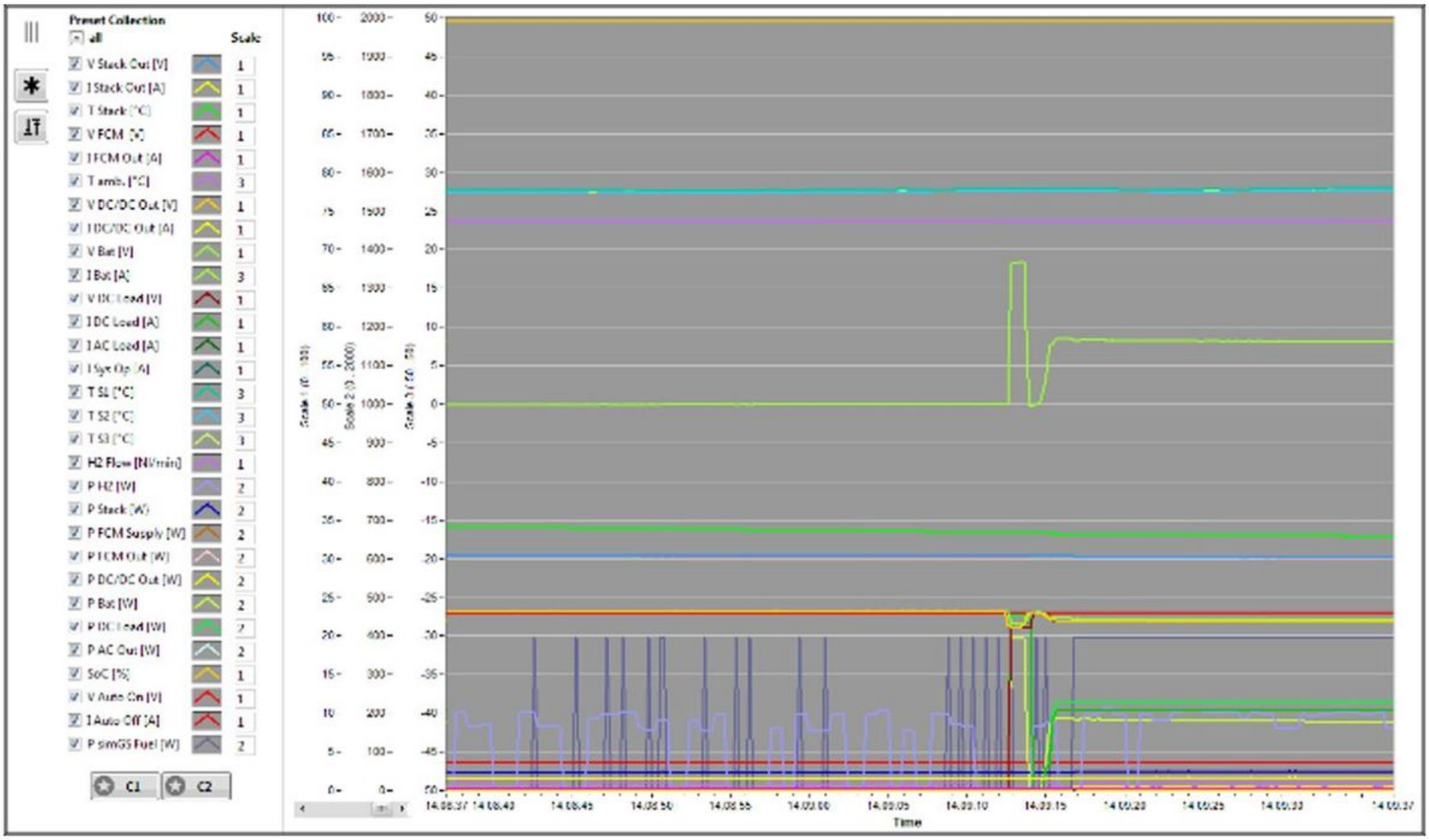

Figure 15

Data acquisition screen.

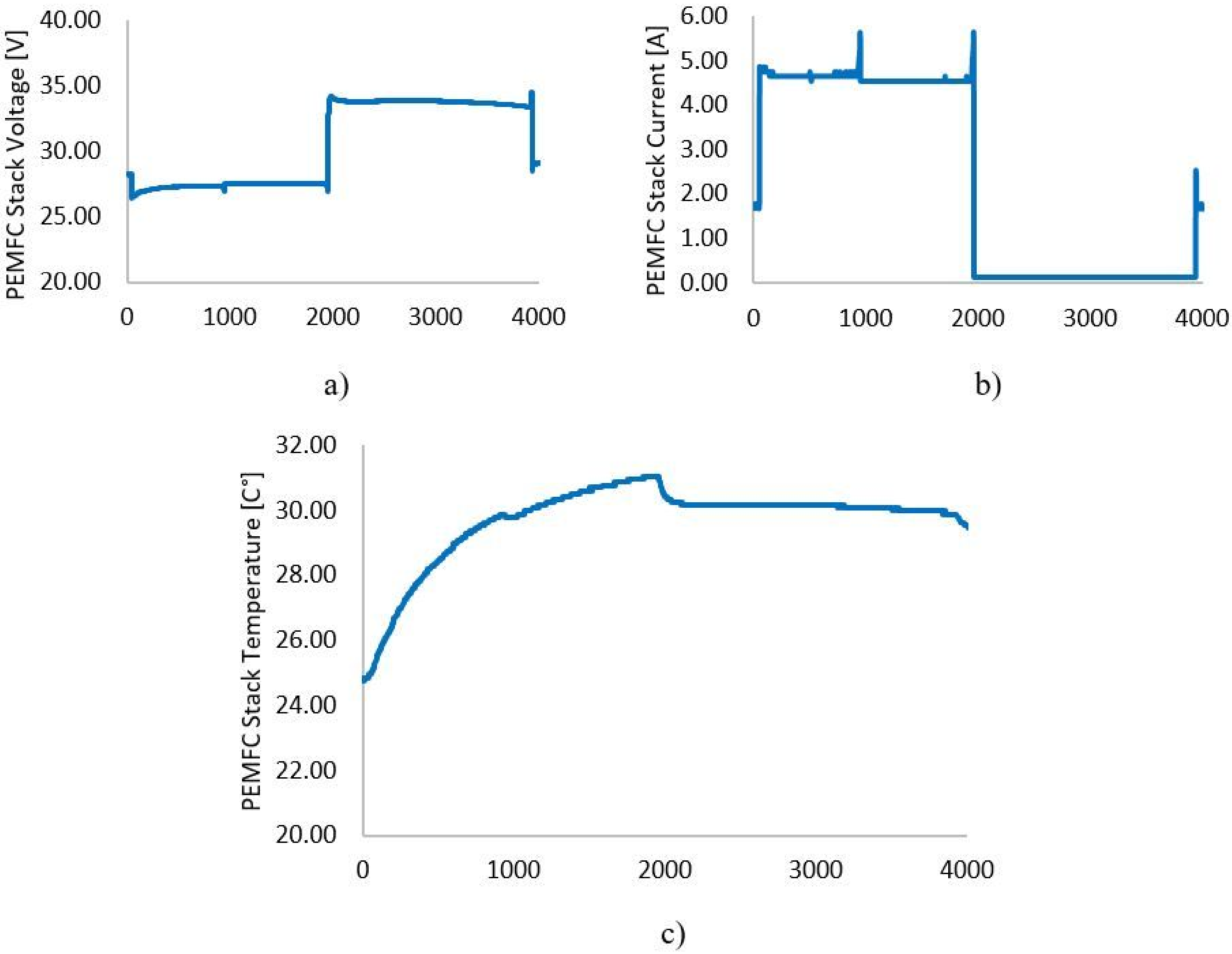

Figure 16

a) PEMFC stack voltage, b) PEMFC stack current, c) PEMFC stack temperature [C°].

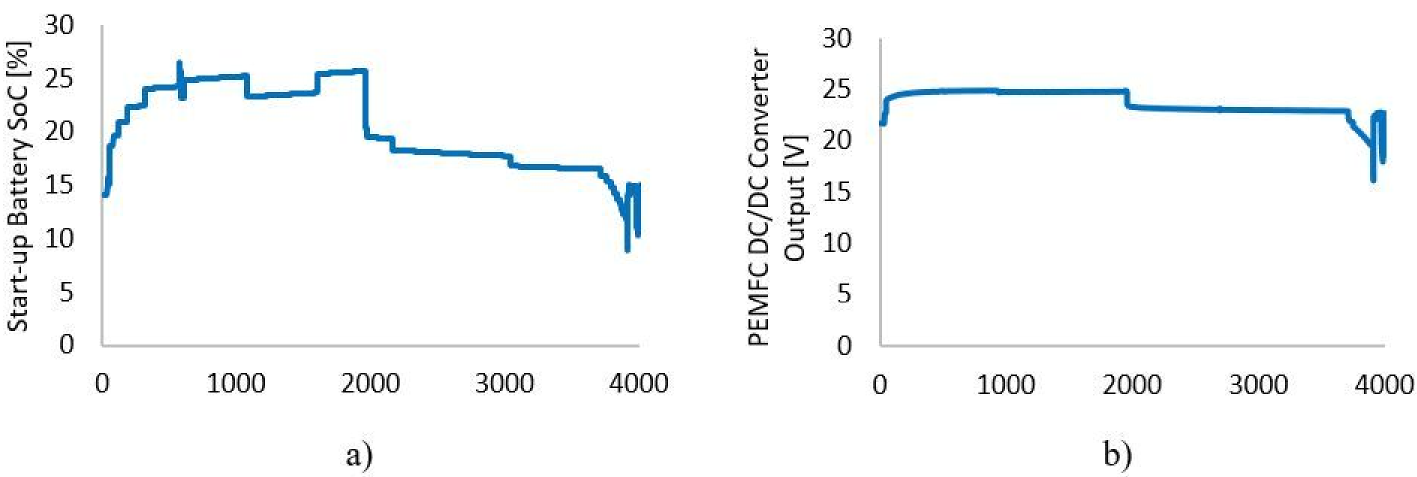

Figure 17

a) Start-up battery state of charge (SoC) levels, b) PEMFC's DC/DC converter output voltages

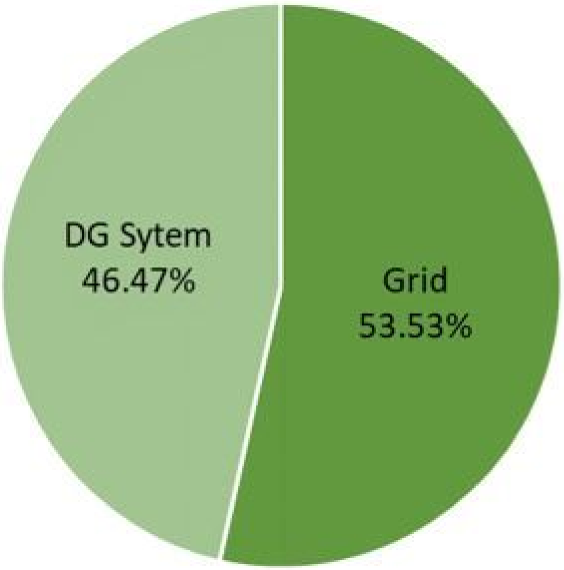

Figure 18

Grid support and DG energy produce.

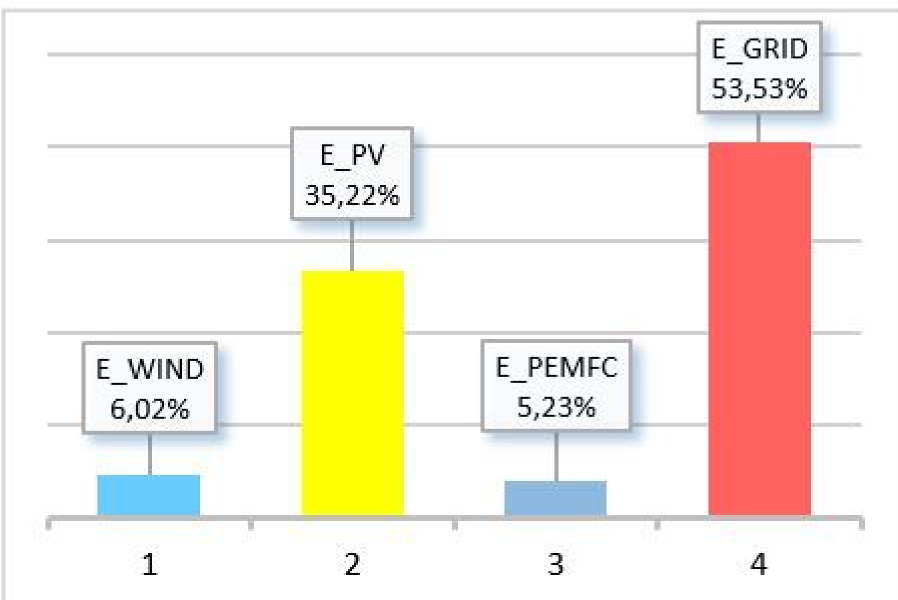

Figure 19

The pie chart of power generation and grid support rates of the microgrid for a defined operation.